

Annual Report

Authors

Ron Adamson
Fremont, CA, USA

Friedrich Garzarolli
Fürth, Germany

Charles Patterson
Clovis, CA, USA

Peter Rudling
ANT International, Mölnlycke, Sweden

Alfred Strasser
Sleepy Hollow, NY, USA

Kit Coleman
Deep River, ON, Canada

Clément Lemaignan
Voreppe, France



A.N.T. INTERNATIONAL®

© December 2011

Advanced Nuclear Technology International
Analysvägen 5, SE-435 33 Mölnlycke
Sweden

info@antinternational.com
www.antinternational.com

Disclaimer

The information presented in this report has been compiled and analysed by Advanced Nuclear Technology International Europe AB (ANT International®) and its subcontractors. ANT International has exercised due diligence in this work, but does not warrant the accuracy or completeness of the information.

ANT International does not assume any responsibility for any consequences as a result of the use of the information for any party, except a warranty for reasonable technical skill, which is limited to the amount paid for this assignment by each ZIRAT/IZNA programme member.

Contents

1	Introduction (Peter Rudling)	1-1
2	BU achievements and key fuel performance issues (Alfred Strasser)	2-1
2.1	Introduction	2-1
2.2	Trends in fuel operating conditions	2-1
2.2.1	General trends	2-1
2.2.2	Fuel cycles	2-2
2.2.3	BU extension	2-5
2.2.4	Power uprates	2-7
2.3	Fuel reliability	2-7
2.3.1	Overall failure rates	2-7
2.3.2	Failure causes – PWRs	2-10
2.3.3	Failure causes – BWRs	2-15
2.4	HB fuel performance summary	2-17
2.4.1	HBs achieved in utility power plants	2-17
2.4.2	HB UO ₂ and MOX fuel examination results	2-20
2.4.2.1	Fission gas release	2-22
2.4.2.2	Thermal conductivity	2-27
2.4.3	HB PWR zirconium alloy performance	2-30
2.4.3.1	ZIRLO, AXIOM alloys	2-31
2.4.3.2	HANA alloys	2-32
2.4.3.3	M-MDA alloy	2-33
2.4.3.4	E110, E125, E635 Alloys	2-35
2.4.3.5	E110 FR to 75 GWD/MT	2-37
2.4.4	HB transient performance of BWR and PWR fuels	2-40
2.4.5	Effect of hydrogen on zirconium alloy performance	2-44
2.4.5.1	Effect of transients	2-44
2.4.5.2	HPU	2-45
2.4.5.3	Hydride orientation	2-49
2.4.6	FA dimensional stability	2-51
2.5	Fabrication	2-60
2.5.1	UO ₂	2-60
2.5.2	Zirconium alloy ingot melting	2-64
2.5.3	Advanced zirconium alloy development	2-68
2.6	LOCA	2-69
2.6.1	Proposed USNRC rule change	2-69
2.6.2	Experimental simulations of LOCA	2-76
2.6.3	LOCA Modelling	2-81
2.7	RIA	2-82
2.7.1	Proposed USNRC regulations	2-82
2.7.2	Evaluation of differences between test reactor and power reactor RIAs	2-85
3	Microstructure (Clément Lemaignan)	3-1
3.1	Introduction	3-1
3.2	Knowing the microstructure	3-1
3.3	Techniques to study the microstructure	3-2
3.3.1	Analysing the atoms	3-3
3.3.1.1	SIMS	3-3
3.3.1.2	3D Atom probe	3-4
3.3.1.3	X-ray diffraction and related items	3-8
3.3.1.3.1	Sources of photons beams	3-8
3.3.1.3.2	Diffraction conditions	3-8

3.3.1.4	Neutron diffraction	3-9
3.3.1.4.1	Neutron sources and properties	3-9
3.3.1.4.2	Examples of neutron diffraction in Zr alloys	3-10
3.3.1.4.3	Small Angle Scattering (SAS)	3-10
3.3.1.4.4	Technology of TEM and sample preparation	3-13
3.3.2	Elastic interaction of particles with atoms	3-15
3.3.2.1	Electron interactions with matter and atoms	3-15
3.3.2.2	Secondary emission and SEM	3-15
3.3.2.3	Characteristics X-ray emission	3-17
3.3.2.4	Back scattering and EBSD	3-18
3.3.3	Inelastic interactions of particles with atoms	3-19
3.3.3.1	Loss of electron energy (EELS) on TEM	3-19
3.3.3.2	Loss of energy and nuclear reactions	3-20
3.3.3.3	Photon absorption spectroscopy (XANES and EXAFS)	3-21
3.3.3.4	X-ray or neutron absorption and 3D tomography	3-23
3.3.4	Impact of atom environment: Vibration frequency and Mössbauer effect	3-23
3.3.4.1	Raman spectroscopy	3-24
3.3.4.2	Mössbauer spectroscopy	3-25
3.3.5	Other techniques	3-26
3.3.5.1	Thermo-electric power	3-26
3.3.5.2	Other techniques of rare utilizations	3-27
3.3.5.3	Chemical characterization	3-28
3.4	Synthesis and comparisons of the different techniques	3-28
3.5	Conclusions and recommendations	3-34
4	Mechanical properties	4-1
4.1	Trace elements in zirconium alloys (Kit Coleman)	4-1
4.1.1	Introduction	4-1
4.1.2	Capture cross-section for thermal neutrons	4-1
4.1.3	Counting atoms rather than weighing them	4-2
4.1.4	Setting the specification based on nuclear properties	4-2
4.1.5	Role of traces of elements on metallurgical properties of zirconium alloys	4-8
4.1.5.1	Aluminum	4-8
4.1.5.2	Carbon	4-9
4.1.5.3	Chlorine	4-12
4.1.5.4	Hydrogen	4-14
4.1.5.5	Nitrogen	4-15
4.1.5.6	Phosphorus	4-16
4.1.5.7	Silicon	4-18
4.1.5.8	Sulphur	4-19
4.1.5.9	Titanium	4-20
4.1.5.10	Uranium	4-20
4.1.6	Changes during reactor service	4-21
4.1.6.1	Zirconium	4-21
4.1.6.1.1	Thermal neutron capture	4-21
4.1.6.1.2	(n,2n)	4-21
4.1.6.1.3	(n,p)	4-21
4.1.6.1.4	(n,d)	4-21
4.1.6.1.5	(n, α)	4-22
4.1.6.2	Alloying elements	4-22
4.1.7	Conclusion	4-23
4.1.8	Summary	4-23
4.2	Fatigue of Zry – A review (Ron Adamson)	4-23
4.2.1	Introduction	4-23
4.2.2	Stress-based fatigue	4-24
4.2.3	Strain-based fatigue	4-27
4.2.4	Statistical nature	4-31
4.2.5	Experimental	4-32

4.2.6	Fractography	4-37
4.2.6.1	Fatigue in irradiated and un-irradiated Zry	4-41
4.2.6.2	Effect of temperature	4-51
4.2.6.3	Effect of iodine	4-52
4.2.6.4	Effect of hydrogen	4-55
4.2.6.5	Fundamental dislocation phenomena	4-56
4.2.6.6	Fatigue crack growth rate	4-59
4.2.6.6.1	Effect of environment	4-61
4.2.6.7	Bottom line	4-67
4.2.7	Summary	4-67
5	Dimensional stability	5-1
6	Corrosion and hydriding (Friedrich Garzarolli)	6-1
6.1	Mechanistic aspects for corrosion and hydriding of Zr alloys corrosion	6-1
6.1.1	Oxidation mechanism	6-1
6.1.2	Hydrogen uptake mechanism	6-28
6.2	Factors affecting HPU during corrosion of Zr alloys	6-42
6.2.1	Out reactor results	6-42
6.2.2	HPU during corrosion of Zr alloys in reactor loops	6-51
6.2.3	HPU during corrosion of Zr alloys in BWR and RBMK	6-58
6.2.4	HPU during corrosion of Zr Alloys in PWR and CANDU reactor	6-58
6.3	Summary	6-61
7	Primary failures and secondary degradation (Peter Rudling)	7-1
7.1	Debris fretting	7-1
7.1.1	Introduction	7-1
7.2	Remedies	7-5
7.2.1	Introduction	7-5
7.2.2	Plant design and operation improvements	7-5
7.2.2.1	Brunswick	7-5
7.2.2.2	Perry	7-7
7.2.2.3	KKL	7-7
7.2.2.4	W debris trap	7-8
7.2.2.5	AREVA debris trap	7-9
7.2.3	Debris filter	7-10
7.2.3.1	Introduction	7-10
7.2.3.2	PWR	7-10
7.2.3.2.1	Korea Nuclear Fuel (KNF)	7-10
7.2.3.2.2	AREVA – PWR	7-11
7.2.3.2.3	W	7-12
7.2.3.3	BWR	7-14
7.2.3.3.1	Westinghouse Electric Sweden (WES)	7-14
7.2.3.3.2	AREVA	7-15
7.2.3.3.3	GNF	7-17
7.2.3.4	VVER-1000	7-19
7.2.3.4.1	TVSA	7-19
7.2.3.4.2	TVSA-5M	7-20
7.2.3.4.3	TVSA-ALFA	7-21
7.2.4	Recent debris fretting failure cases	7-21
7.2.4.1	BWRs	7-21
7.2.4.2	VVER 440 and 1000 reactors	7-23
7.2.4.3	CANDU	7-30
7.2.4.4	PWRs	7-30
7.3	Summary	7-32

8	Cladding performance under accident conditions LOCA and RIA	8-1
9	Fuel performance during dry storage (Charles Patterson)	9-1
9.1	Introduction	9-1
9.2	Status of interim storage programs	9-6
9.2.1	United States	9-6
9.2.1.1	General status	9-6
9.2.1.2	Summary of regulations	9-10
9.2.2	International	9-13
9.2.2.1	General status	9-13
9.2.2.2	Comparison of international regulations	9-15
9.3	Dry storage conditions relevant to fuel performance	9-17
9.3.1	Overview of storage conditions	9-17
9.3.2	Decay heat and storage temperature	9-19
9.3.3	Cladding stress	9-21
9.3.4	Actinide decay and helium generation	9-22
9.3.5	Creep rupture	9-23
9.3.6	Hydrogen assisted cracking (DHC)	9-23
9.3.7	Fuel and cladding degradation	9-24
9.3.8	SCC	9-24
9.4	Extended storage issues	9-24
9.5	Hydrogen and hydriding	9-26
9.5.1	Background	9-26
9.5.2	Cladding temperature	9-26
9.5.3	HPU	9-28
9.5.4	Hydrogen solubility	9-31
9.5.5	Hydride structure	9-34
9.5.6	Hydride morphology	9-34
9.5.7	Hydrogen migration	9-37
9.5.8	Radial reorientation	9-44
9.5.9	Strength of hydrided material	9-53
9.5.10	Ductility of hydrided material	9-58
9.5.11	Delayed hydrogen cracking	9-63
9.5.12	Conclusions regarding hydrogen and hydriding in dry storage	9-65
9.6	Summary	9-67
10	Trends and needs	10-1
11	References	11-1
	Nomenclature	
	Unit conversion	

1 Introduction (Peter Rudling)

The objective of the Annual Review of ZIRconium Alloy Technology (ZIRAT) and Information on Zirconium Alloys (IZNA) is to review and evaluate the latest developments in ZIRAT as they apply to nuclear fuel design and performance.

The objective is met through a review and evaluation of the most recent data on zirconium alloys and to identify the most important new information and discuss its significance in relation to fuel performance now and in the future. Included in the review are topics on materials research and development, fabrication, component design, and in-reactor performance.

Within the ZIRAT16/IZNA11 Program, the following technical meetings were covered:

- 16th International Symposium on Zirconium in the Nuclear Industry, Chengdu, Sichuan, China, May 9–13, 2010
- Jahrestagung Kerntechnik, Germany, May 17-19, 2011
- Water Reactor Fuel Performance Meeting (WRFPM), Chengdu, China, September 11–29, 2011
- 9th International Conference on VVER¹ Fuel Performance, Bulgaria, September, 19- 23, 2011
- NACE² International, Corrosion 2011 Conference and Expo

The extensive, continuous flow of journal publications is being monitored by several literature searches of worldwide publications and the important papers are summarised and critically evaluated. This includes the following journals:

- Journal of Nuclear Materials
- Nuclear Engineering and Design
- Kerntechnik
- Metallurgical and Materials Transactions A
- Journal of Alloys and Compounds
- Canadian Metallurgical Quarterly
- Journal de Physique IV
- Journal of Nuclear Science and Technology
- Nuclear Science & Engineering
- Nuclear Technology

The primary issues addressed in the review and this report is zirconium alloy research and development, fabrication, component design, ex- and in-reactor performance including:

- Regulatory bodies and utility perspectives related to fuel performance issues, fuel vendor developments of new fuel design to meet the fuel performance issues.
- Fabrication and Quality Control (QC) of zirconium manufacturing, zirconium alloy systems.

¹ Voda Voda Energo Reactor (Russian type PWR)

² National Association of Corrosion Engineers

- Mechanical properties and their test methods (that are not covered in any other section in the report).
- Dimensional stability (growth and creep).
- Primary coolant chemistry and its effect on zirconium alloy component performance.
- Corrosion and hydriding mechanisms and performance of commercial alloys.
- Cladding primary failures.
- Post-failure degradation of failed fuel.
- Cladding performance in postulated accidents (Loss of Coolant Accident (LOCA), Reactivity Initiated Accident (RIA)).
- Dry storage.
- Potential Burnup (BU) limitations.
- Current uncertainties and issues needing solution are identified throughout the report.

Background data from prior periods have been included wherever needed. The data published in this Report is only from non-proprietary sources; however, their compilation, evaluations, and conclusions in the report are proprietary to ANT International and ZIRAT/IZNA members as noted on the title page.

The authors of the report are Dr. Ron Adamson, Mr. Al Strasser, Mr. Friedrich Garzarolli, Dr. Charles Patterson and, Dr. Kit Coleman and, Mr. Peter Rudling, President of ANT International.

The work reported herein will be presented in two Seminars: in Clearwater Beach, FL., USA (February 6–8, 2012), in St Julien, Malta, Europe (March 7–9, 2012).

The Term of ZIRAT16/IZNA11 started on February 1, 2011 and ends on March 31, 2012.

2 BU achievements and key fuel performance issues (Alfred Strasser)

2.1 Introduction

The objective of this Section is to summarize the key performance issues that could affect fuel design, fabrication or operation of the nuclear fuel in the near term or the longer term. Topics covered include the fuel itself and all the Fuel Assembly (FA) components made of zirconium alloys nickel base alloys and stainless steels. The information sources reviewed, screened and evaluated include nearly all the related publications and technical meeting presentations of the past, approximately 18 months and focuses primarily on extended BU data. The Section is intended to be a guide to significant, current issues and provide an alert to items that could affect fuel related operations. The extensive volume of information involved limits the presentations to the most significant features and conclusions, and the reader is urged to refer to the referenced publications and the ZIRAT/IZNA Annual Reports(ARs) or Special Topical Reports for more detailed back-up data on topics of interest.

2.2 Trends in fuel operating conditions

2.2.1 General trends

Improved fuel reliability and operating economics are the driving forces for the changes in operating conditions, while maintaining acceptable margins to operating and regulatory safety limits. These are incentives for significant advances in materials technology, software for modelling fuel performance, sophisticated instrumentation and methods for post-irradiation examinations. Some of these advances in technology have increased the demands on fuel performance levels and put pressure on the regulatory bodies to license operations to increased BU levels. The types of changes in Light Water Reactor (LWR) operating methods intended to achieve improved safety and economics have not changed in the past years and still include:

- Annual fuel cycles extended to 18 and 24 months,
- Increased discharge BUs to 58 GWD/MT batch average exposures by higher enrichments, increased number of burnable absorbers in the assemblies and in Pressurized Water Reactors (PWRs) higher Li and B levels in the coolant, or enriched B in the coolant,
- Plant power uprates that range from 2 to 20%,
- More aggressive fuel management methods with increased enrichment levels and peaking factors,
- Reduced activity transport by Zn injection into the coolant,
- Improved water chemistry controls and increased monitoring,
- Component life extension with Hydrogen Water Chemistry (HWC) and Noble Metal Chemistry (NMC) in Boiling Water Reactors (BWRs).

2.2.2 Fuel cycles

Cycle lengths

The trend for increased fuel cycle lengths has come to a near “equilibrium” in the US with PWRs operating at an average of 500 Effective Full Power Days (EFFPD) per cycle and BWRs an average of 620 EFFPD per cycle, up to a maximum of about 680 days for PWRs and 720 days for BWRs (Figure 2-1). Nearly all the US BWRs are trending toward 24 month cycles. The older, lower power density PWRs have implemented the 24 month cycles, but fuel management limitations, specifically the reload batch sizes required, have limited implementation of 24 month cycles in the high power density plants. Nevertheless, some high power PWRs, such as Diablo Canyon, are considering 24 month cycles, the incentive being one less shutdown per 5 years. Their planned approach is to change from the Westinghouse (W) Optimized Fuel Assembly (OFA) fuel to the larger diameter robust fuel. This will provide a larger amount of uranium per reload and permit reloads that are smaller than the ½ core that OFA fuel would require. The economics of 24 month cycles tend to become plant specific since they depend on the balance of a variety of plant specific parameters. The potential economic gains for cycle extension have decreased in the US as the downtimes for reloading and maintenance procedures were significantly reduced.

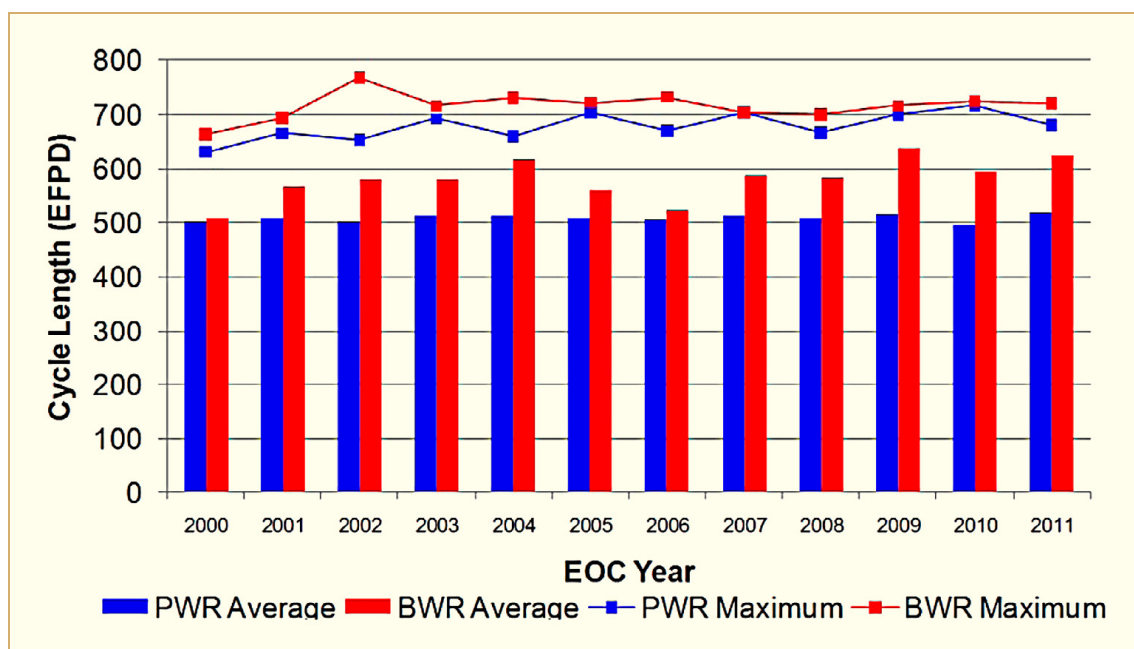


Figure 2-1: Average US cycle length trends [Daum, 2011].

Other countries that historically have had only one peak power demand per year in the winter, compared to the two summer and winter power peaks in the US, are also trending toward longer cycles as a result of changes in economics, maintenance practices and licensing procedures. PWRs are trending toward 18 month cycles in France, Belgium and Germany.

Capacity factors

The median capacity of the US plants has been about 90% for the period of 2002 to 2010. The mean factors for the BWRs and PWRs have been nearly identical varying less than 1% differential. The spread between the top and bottom quartile plants as a function of years is given in Figure 2-2 and shows that the top quartile has been above 92% consistently over the past 11 years and the bottom quartile has improved except for a slight slip in the recent years. This shows that the current good performance has plateaued out, but further improvements will be attempted.

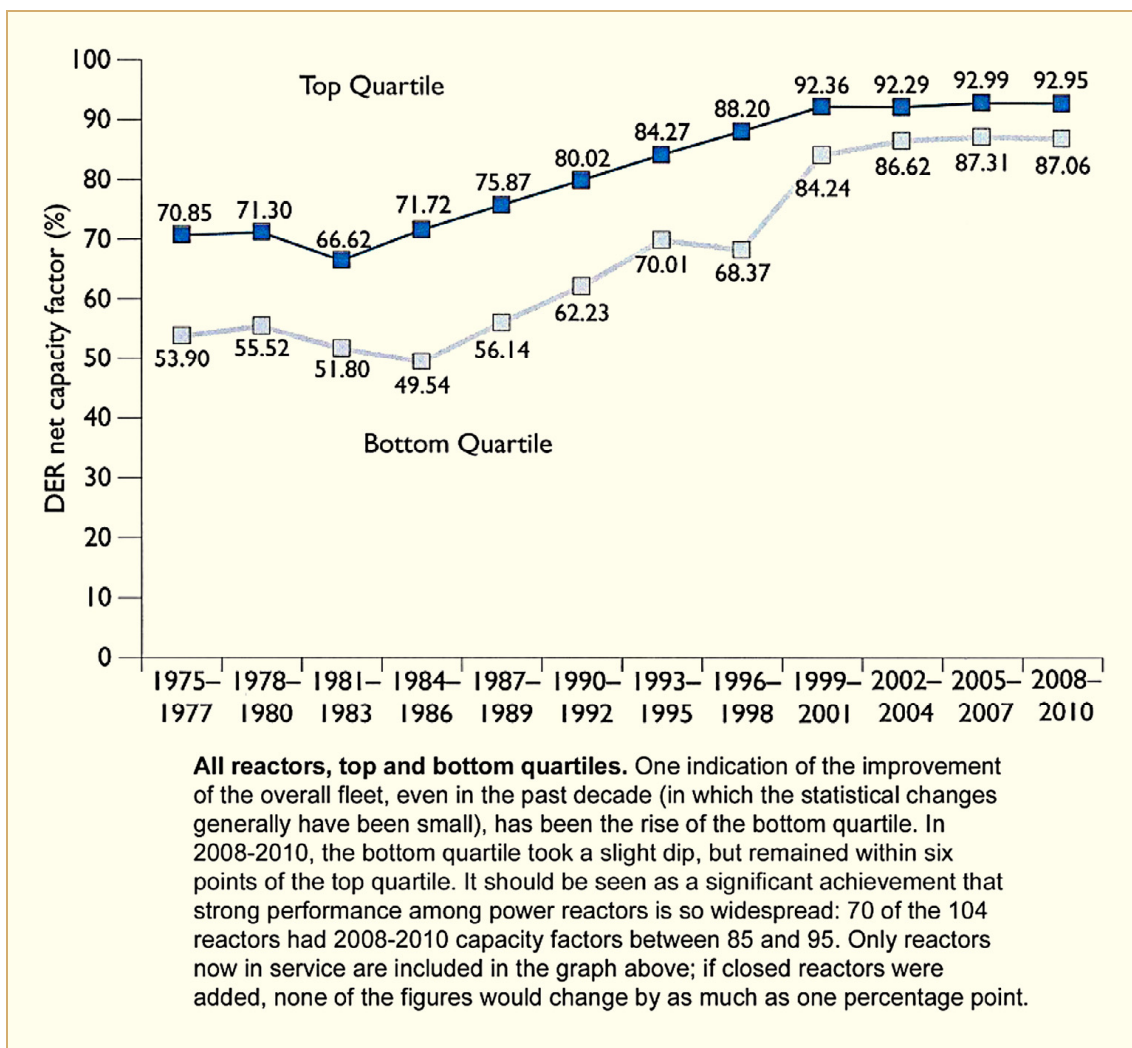


Figure 2-2: Improvement of US plant capacity factors [Blake, 2011], (DER=median 3 year design electrical rating).

Spent fuel storage

The Blue Ribbon Commission (BRC) on America's Nuclear Future issued its draft report for public comment by October 31, 2011. The report does not offer a practical solution to supplant Yucca Mountain, but does say that the US has an obligation to find a solution to deal with spent fuel. The proposed strategy to deal with this was expressed in several points:

- A new, consent based approach to siting future nuclear waste management facilities,
- A new organization dedicated solely to implementing the waste management program and empowered with authority and resources to succeed,
- Access to the funds utility rate payers are providing for nuclear waste management,
- Efforts to develop one or more geologic disposal and interim storage facilities,
- Support continued US innovation in nuclear technology and workforce development,
- Active US leadership in international activities to address safety, waste management, non-proliferation and security concerns.

3 Microstructure (Clément Lemaignan)

3.1 Introduction

The aim of this section is to provide to the readers a background survey of the techniques used for the knowledge of the microstructure in metallurgy, with special emphasis in connection to Research & Development (R&D) for zirconium and its alloys. Since the techniques currently available to the scientists are more and more advanced, with the use of very sophisticated equipments, and since the distance between what is measured and how the results are presented is increasing steadily, a basic knowledge of the actual physics leading to a number or an image is required to feel what is the “transfer function” between the observation and the reality, and therefore the understanding of the value of the results, their limits (accuracy, sensibility, repeatability) or any possible artefacts.

Avoiding long technological developments, easily found in numerous reference textbooks [ASM International, 1992], we would provide “hand-on” descriptions of the techniques that have been used in the recent scientific studies published in the scientific field of Zr alloy microstructure. For each of the techniques to be described, the physical background will be presented, the limitations²⁶, the risks of misinterpretations or known errors will be discussed and a table of main characteristics will be given. Examples of results published recently will illustrate how specific a given technique can be and its interest for solving a precise question.

3.2 Knowing the microstructure

The microstructure is defined as the structure at the microscopic scale. The structure of a thing describes how the parts of this thing relate to each other, how they are “assembled”. The microscopic scale is the one that requires a magnification device to be observed, and is conventionally defined as what is observed at a 25 x scale. Therefore the techniques related to naked eye observation (macrostructure) or assemblies, will not be covered in this section. Similarly, the subatomic scale remains outside the scope of this review. The only matter of concern, at this scale, will be the oxidation state of each atom.

In metallurgy, the knowledge of the microstructure is a mandatory requirement, and has always been requested with the highest accuracy as possible. At the beginning of the metallurgy optical microscopy and X-ray diffraction were used as routine tools as soon as they were available. It has been the same for more modern techniques such as Transmission Electron Microscope (TEM), neutron diffraction and atomic chemistry tools (Secondary Ion Mass Spectroscopy (SIMS), 3D tomography), to be described later.

The reason for knowing the microstructure is due to the fact that the properties of the alloys are strongly microstructure dependent. With the same composition, the microstructure of an alloy can be deeply changed, depending of its thermomechanical history. Heat treatments, mechanical processing, conditions of use (a very important point in our case due to the effects of irradiation on the microstructure) induce major changes in the microstructure, inducing large changes in all the properties. Limiting our topic to engineering properties, mechanical strength, fracture toughness, corrosion resistance, creep etc. are known to depend on the microstructure.

Bridging a link between the microstructure and the properties allows the scientists to understand the mechanisms involved in the control of the property under consideration. This opens the route to improvements in the properties of the alloys and/or allows the designers to forecast changes in properties during operation (e.g. irradiation hardening or growth, changes in corrosion resistance after heat treatments).

²⁶ American Society of Metals

Using the definition given above, the question to be solved with respect to the microstructure is to know what are the “parts” to be considered in the way they “relate to each other”. For the microstructures of interest, three major elements have to be considered:

- The crystals are the elementary units of the metals and alloys. One has to know what is the crystallographic structure (crystallographic system, composition), what is the shape of each crystal (elongated, equiaxed), what is their relative orientation (occurrence of a crystallographic texture).
- Within the crystals, the defects have to be described accurately. Among them, we have to consider chemical defects such as clusters of foreign or solute atoms, linear defects (dislocations) and point defects (irradiation defects such as interstitials or vacancies, or chemical defects – substitutional or interstitial impurities).
- At the atomic scale, the exact chemical state and chemical environment of each atom controls its behaviour. Of interest are the oxidation state, the surrounding atoms controlling the vibration modes and therefore the mobility.

3.3 Techniques to study the microstructure

Having in mind the questions raised above, any physical phenomenon whose characteristic parameters would be affected, in any possible way, by the microstructure will lead to final results affected by the microstructure, and therefore could be used for its analysis. Since “Any physical property or quantity measurable in a system is related, in one way or another, to all the other variables of the system” [Avril, 1974], one can consider that any physical phenomenon could be used for the analysis of the microstructure of alloys. However, practical considerations limit the techniques of actual interest. Indeed, accuracy, selectivity, uniqueness of the relationship between the parameter to be analysed and the microstructure and the output of the physical experiment, or cost or complexity of the measurements limit the list to a set of basic phenomena to be considered.

Sorting the different techniques used in metallurgy for the knowledge of the microstructure is a rather difficult task for the reason that any phenomenon that could give any information could be used, at least a-priori. Indeed the imagination of the scientists is large enough that experiments have been reported where the interest, the relevance or the understanding of the work could remain questionable to the rest of the scientific community. Therefore, we will limit ourselves to the techniques for which a common agreement exists on the interest, the applicability and the usefulness.

With respect to the physical basis of the physics of concern, the techniques could be categorised as follows:

- Direct measurement of each atom, giving its mass, chemistry and location in the sample. This category includes the SIMS, and the 3D atom microprobe.
- Diffraction induced by the periodic (crystallographic) nature of the grains. Any beam whose wavelength is commensurate with the interatomic distance will exhibit diffraction phenomena. Among them, X-rays, electrons, neutrons can be used for this purpose. Low angles diffraction will also be described in this section.
- Interactions of particles with the atoms, either in-elastically:
 - TEM and analysis in the TEM by Electron Energy Loss Spectroscopy (EELS),
 - Electron probe micro-analysis (EPMA),
 - Neutron radiography,
 - All the nuclear microprobe techniques, including Proton Induced X-ray Emission (PIXE),
 - or the phenomena driven by inelastic interactions, such as the surface imaging obtained by SEM.

- Another interesting group of techniques is based on the change in reaction of an atom to an external excitation, according to its chemical environment. X-ray absorption near the characteristics absorption energies: Extended X-Ray Absorption Fine Structure (EXAFS) and variant such as X-Ray Absorption Near Edge Spectroscopy (XANES). The dependence of the vibration frequencies of an atom with its environment can be analysed indirectly with Infrared (IR) photons, such as the Raman spectroscopy, or with γ rays (Maussbauer spectroscopy).

3.3.1 Analysing the atoms

Two techniques are available for the knowledge of the microstructure at the atom scale. In the two cases, the processes require the following steps: extraction of the atoms from the sample, ionising it in order to perform its chemical analysis with e/m spectroscopy, and reconstruction as 2D or 3D chemical maps.

3.3.1.1 SIMS

The principle of the SIMS is given in Figure 3-1. A sample is bombarded with an ion gun focussed at the surface and/or sweeping it. The incoming ions (Cs^+ , O^- , Ar^+ , Ga^+ , O_2^+), accelerated to energies of a few tens of keV, induce damage to the surface and the displacement cascades sputter the surface atoms out. The sputtering yield is low for pure metals without oxygen, but can be increased by a factor of 10^3 - 10^4 with O additions.

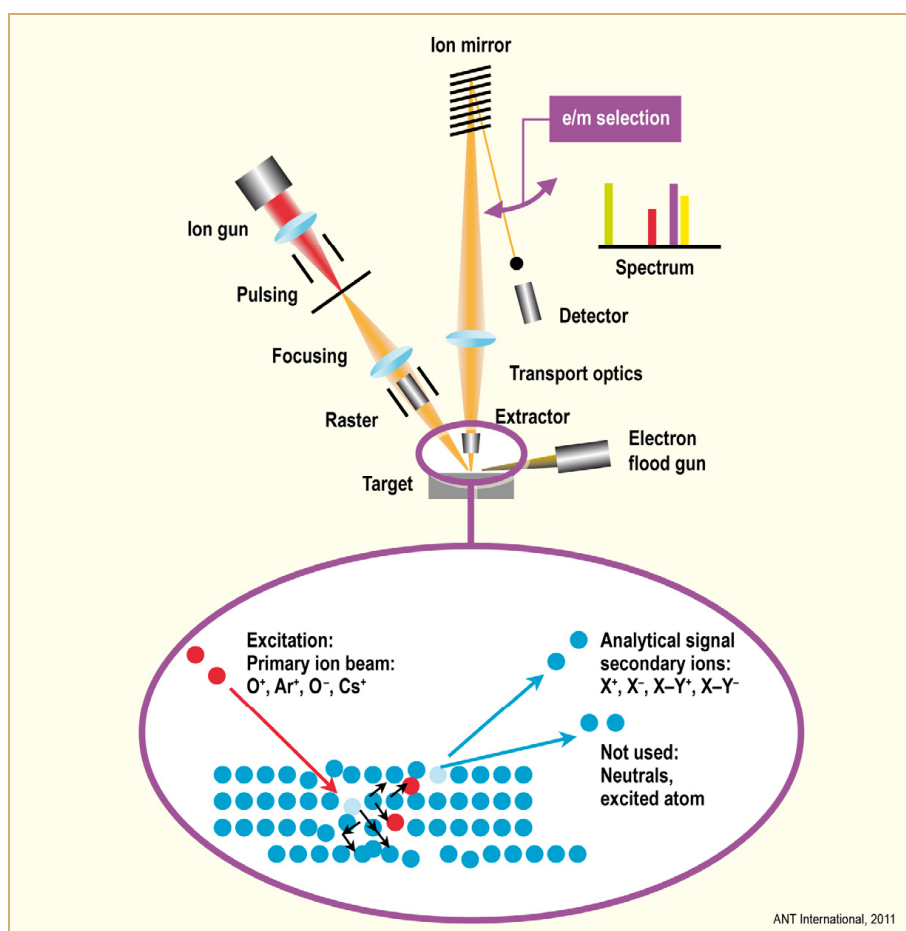


Figure 3-1: Schematic of the SIMS.

4 Mechanical properties

4.1 Trace elements in zirconium alloys (Kit Coleman)

4.1.1 Introduction

“The influence exerted by a small quantity of metallic or other impurity on a mass of normal metal is shown by a remarkable series of phenomena. The valuable mechanical properties conferred upon metals by associating them with small, but definite, amounts of other metals constitute the main reason why metals devoted to industrial use are seldom employed in a state of purity”.

This quotation is from a paper written in 1888 by W. C. Roberts-Austen (who gave his name to Austenite) during his study of the properties of gold [Roberts-Austen, 1888]. He in turn quotes Bergman who in 1781 demonstrated the critical role of carbon on the properties of iron, expressing “his astonishment at the smallness of the amount of carbon capable of producing such effects” [Bergman, 1783]. Thus the effects of trace elements on the behaviour of metals have been a source of both improvement and decline in properties for over two hundred years. This essay is an overview of trace elements in zirconium alloys. A brief history lesson leads into alloy specification and examples of controlling small concentrations of some elements.

4.1.2 Capture cross-section for thermal neutrons

Early in the development of thermal nuclear reactors it was recognised that for high efficiency of the fission process the number of thermal neutrons absorbed by structural materials should be as low as possible. A cross-section represents the probability of a reaction between the atomic nucleus of the metal and the impinging particle and has the dimensions of area. The cross-section for a single nucleus is the microscopic cross-section, σ . Since the heavy nuclei have diameters of about 10^{-12} cm then it is not surprising that σ for many elements is about 10^{-24} cm². This number is often called a “barn” or b. The macroscopic cross-section, Σ , represents the cross-section of all the nuclei, N , in a standard volume, N/cm^3 ; it has the dimensions of a reciprocal length because $\Sigma = \sigma N \text{ cm}^2/\text{cm}^3$. For an element

$$\text{Eq. 4-1:} \quad \Sigma = \sigma \rho N_0 / A_E$$

where ρ = density of the element,
 A_E = atomic weight of the element, and
 N_0 = Avogadro’s number.

For an alloy, Σ must be summed for the number of atoms of each element present.

In the ‘40s, at the conceptual stage of thermal reactor development, zirconium did not look promising as a structural material; it was expensive to produce, very little was available and it appeared to have a large value of σ , about 6.8 b [Havers et al, 1947]. These measurements also indicated that hafnium had a very high value of σ [Ross & Story, 1948/1949]. Zirconium ores usually contain about 2 wt.% hafnium that were thought to contribute to the apparent value of σ for zirconium. Once the hafnium was much reduced, the true value of σ of about 0.18 b, was revealed [Pomerance, 1951], a value of σ of 1.52 b for the isotope Zr91, which makes up 11.2 % of the natural isotopes, contributes most of the value of σ for the element [Pomerance, 1952]. Hafnium is the first example of an important trace element whose concentration must be controlled. For nuclear applications, hafnium reduction is a key part of the fabrication process of components and several methods are available, for example Methyl Isobutyl Ketone- ammonium Thiocyanate (MIBK-Thiocyanate) Process [Fischer & Chalybaeus, 1947], [Fischer et al, 1948].

Very pure zirconium could be made by the van Arkel-de Boer iodide process to make small quantities of costly “crystal bar” zirconium. Once the good nuclear property was established, methods of extraction and refinement based on the Kroll process for titanium were developed in the US in the late ‘40s and early ‘50s to produce a form of the metal called sponge zirconium. Sponge zirconium was less pure than crystal bar, but the price was reduced by a factor of about 50 and the quantities of metal available for components were increased from a few kilograms to several 100 Mg. Various shapes suitable for components could be fabricated from sponge zirconium with attendant acceptable mechanical properties. A little later, in Russia, similar production was in progress by developing the molten salt electrolysis process to make zirconium powder in large quantities.

Zirconium of high purity is corrosion resistant in HT water. Unalloyed sponge zirconium exhibited variable corrosion behaviour in water and steam, which was attributed to variations in the concentration of trace impurities. The effort to improve corrosion resistance is partly based on alloying and partly based on controlling the amount and distribution of these trace elements. Once the true nuclear properties of zirconium were realised and production of large quantities of metal was possible, alloy and specification development aimed at maintaining the nuclear properties and improving corrosion resistance and mechanical properties. This essay focuses on the nuclear and metallurgical properties affected by trace elements. The iterative interaction between resolution of chemical analysis and fabrication processes designed to control small concentrations of elements are not treated in detail. Each plays a role in defining a limit on concentration: what can be achieved by refining and what are the limits of chemical analysis, plus some margin.

4.1.3 Counting atoms rather than weighing them

As indicated in the Introduction, it is the number of atoms rather than their weight that is important for thermal neutron capture cross-sections. Also, for many metallurgical properties involving different compositions, atomic percentage or atom fraction should be used to make sense of correlations with concentration of alloying or trace elements; unfortunately, such is not the usual practice. To apply Eq. 4-1 for σ_A of zirconium containing other elements, we need to convert concentrations of the element in weight, w_E , to concentrations in atom fraction of the element, a_E , through:

$$\text{Eq. 4-2:} \quad a_E = (w_E/A_E)/(w_E/A_E + w_{Zr}/A_{Zr})$$

4.1.4 Setting the specification based on nuclear properties

Table 4-1 includes most of the periodic table of the elements listed in order of macro-cross-section contribution (based on Eq. 4-1 and data from the List of the Elements in Wikipedia) and provides the total macro-capture cross-section of a hypothetical zirconium alloy with an atomic fraction of 0.002 of each element. The right-hand column compares the cross-section of the binary alloy with pure zirconium. Of the elements that *decrease* the cross-section of a zirconium alloy, only oxygen is useful. With a concentration of 0.002 atomic fraction of oxygen the decrease in cross-section is very small – about 0.2%. All the other elements *increase* the cross-section. Up to nickel the increase is 10% or less, while beyond hafnium the increase is over 100%. These results provide a first guideline for alloy development and which elements to avoid, even in trace quantities.

Table 4-1: Contribution to neutron capture cross-section of elements in zirconium containing 0.002 atomic fraction of each element.

Element	Micro-cross-section barns	Density gm/cm ³	Atomic weight	Macro-cross-section cm ² /cm ³	Constant specification atomic fraction	Cross-section of Zr + element	(Zr+spec)/Zr
Fluorine	0.0096	0.0017	19.0	0.0000001	0.002	0.00789	0.99800
Oxygen	0.00019	0.00143	16	0.0000001	0.002	0.007892	0.99804
Hydrogen	0.333	0.00009	1	0.000018	0.002	0.007892	0.99805
Nitrogen	1.91	0.00125	14.0	0.0001	0.002	0.007892	0.99807
Carbon	0.0035	2.27	12.0	0.00040	0.002	0.00789	0.9981
Polonium	0.03	9.32	209.0	0.00081	0.002	0.00789	0.9982
Bismuth	0.034	9.81	209.0	0.00096	0.002	0.00789	0.9982
Beryllium	0.0092	1.85	9.01	0.00114	0.002	0.00789	0.9983
Chlorine	35.5	0.0032	35.46	0.00194	0.002	0.00790	0.9985
Magnesium	0.063	1.74	24.3	0.0027	0.002	0.00789	0.9987
Rubidium	0.38	1.53	85.5	0.0041	0.002	0.00789	0.9990
Lead	0.171	11.34	207.2	0.0056	0.002	0.00790	0.9994
Phosphorus	0.172	1.82	31.0	0.0061	0.002	0.00790	0.9995
Zirconium	0.184	6.51	91.2	0.0079	0.002	0.00790	1.0000
Silicon	0.171	2.33	28.1	0.0085	0.002	0.00790	1.0002
Calcium	0.43	1.54	40.1	0.0099	0.002	0.00791	1.0005
Sodium	0.53	0.971	23.0	0.0135	0.002	0.00791	1.0014
Aluminum	0.232	2.70	27.0	0.0140	0.002	0.00791	1.0015
Cerium	0.6	6.77	140.1	0.0175	0.002	0.00792	1.0024
Barium	1.3	3.59	137.3	0.0205	0.002	0.00793	1.0032
Sulphur	0.53	2.07	32.1	0.0206	0.002	0.00793	1.0032
Tin	0.626	7.29	118.7	0.0231	0.002	0.00793	1.0039
Strontium	1.28	2.64	87.6	0.0232	0.002	0.00793	1.0039
Potassium	2.1	0.86	39.1	0.0279	0.002	0.00794	1.0051
Yttrium	1.28	4.47	88.9	0.0387	0.002	0.00796	1.0078
Platinum	0.96	21.46	195.1	0.0636	0.002	0.00801	1.0141
Niobium	1.15	8.57	92.9	0.0639	0.002	0.00801	1.0142
Zinc	1.11	7.13	65.4	0.0729	0.002	0.00803	1.0165
Germanium	2.2	5.32	72.6	0.0971	0.002	0.00808	1.0226
Thallium	3.43	11.85	204.4	0.1198	0.002	0.00813	1.0283
Tellurium	4.7	6.23	127.6	0.1382	0.002	0.00816	1.0330
Gallium	2.9	5.91	69.7	0.1480	0.002	0.00818	1.0354
Bromine	6.8	3.12	79.9	0.1600	0.002	0.00821	1.0385
Antimony	4.91	6.69	121.8	0.1623	0.002	0.00821	1.0391
Molybdenum	2.6	10.22	96.0	0.1668	0.002	0.00822	1.0402
Ruthenium	2.56	12.37	101.1	0.1886	0.002	0.00826	1.0457
Arsenic	4.3	5.78	74.9	0.1996	0.002	0.00829	1.0485
Iron	2.56	7.87	55.8	0.2174	0.002	0.00832	1.0530
Lanthanum	8.98	6.15	138.9	0.2392	0.002	0.00837	1.0585
Caesium	29	1.87	132.9	0.2461	0.002	0.00838	1.0603
Chromium	3.1	7.15	52.0	0.2567	0.002	0.00840	1.0630

ANT International, 2011

5 Dimensional stability

A limited amount of information was published on this topic during the last 18 months. Dimensional stability will be covered in ZIRAT17/IZNA12 (next year).

6 Corrosion and hydriding (Friedrich Garzarolli)

6.1 Mechanistic aspects for corrosion and hydriding of Zr alloys corrosion

In the following the state of knowledge on the mechanism of corrosion and HPU is given considering especially the recent publications as an update to the information that was given in ZIRAT9-13/IZNA4-8 ARs by Brian Cox and ZIRAT12/IZNA7 STR on Corrosion Mechanism and ZIRAT13 STR/IZNA8 on Effect of Hydrogen on Zr Alloy Properties.

6.1.1 Oxidation mechanism

Corrosion kinetics

Zirconium and its alloys are highly reactive and react at ambient temperatures with oxygen-containing environments and become usually covered by an air-formed passive oxide film that is ~2 nm thick. At higher temperatures the oxide layer increases significantly with increasing exposure time. Figure 6-1 presents a simplified view of the corrosion kinetics in pressurized water, an approximately cubic pre-transition growth law followed by a sharp transition, when an oxide thickness of 1.5-3 μm has been reached to an approximately linear post-transition corrosion rate.

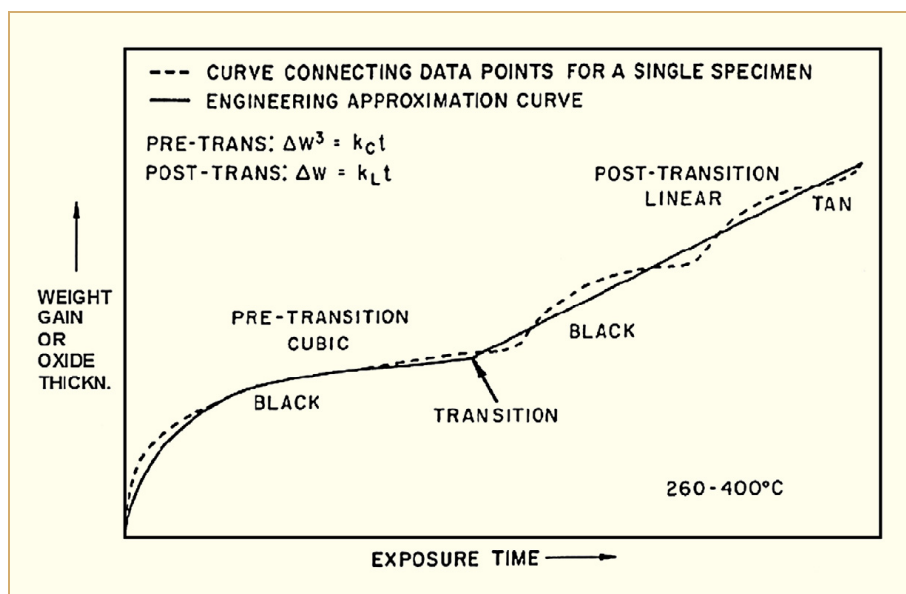


Figure 6-1: Schematic representation of the corrosion behaviour of Zry-4 in the temperature range 260-400°C [Hillner, 1977].

Out of reactor, in oxygen free water, the corrosion forms at first a dense protective oxide film. Initially, the corrosion kinetics in the temperature range on 250-400°C follows an approximate cubic law (Figure 6-1), the rate decreases with increasing oxide layer thickness, S , and time, t .

$$\text{Eq. 6-1: } S^3 = k \cdot t$$

where S is oxide layer thickness,
 t is time, and
 k is a constant.

The corrosion rate (ds/dt) before and after the rate transition shows an exponential temperature dependence.

For the post transition corrosion rate, which is most important for in-PWR corrosion modelling the following equation is used:

$$\text{Eq. 6-2:} \quad ds/dt = C \cdot \exp(-Q/RT),$$

where C is the corrosion constant that depends on Zr-alloy composition and final heat treatment condition,

Q is the activation energy,

R is the gas constant,

T is the absolute temperature.

The temperature effect on corrosion rate is related to the increased transport rate of the corrosion species (electrons and/or oxygen ions) responsible for the oxide growth with increased temperature. The activation temperature, Q/R , is reported to be between 11000 and 16000 K and appears to be quite independent of the Zr-alloy composition and final heat treatment condition.

This general model for the out-of-reactor corrosion process in oxygen free water is widely accepted, although it was pointed out, e.g. [Bryner, 1979] that the quasi-linear corrosion is in reality a periodic corrosion behaviour, repeating the first stage of oxide growth and transition at least at short to intermediate exposure times, see Figure 6-1.

A remarkable periodic repetition of certain features in oxide structure with distance from the metal/oxide interface was observed with different techniques, e.g. [Motta et al, 2005]. Optical microscopy and SEM showed lateral cracks (Figure 6-2) developed in the oxide with a certain periodicity. Also, variations of grain shape (columnar and equiaxed) X-ray peak intensities for both monoclinic and tetragonal zirconia, and texture were observed with distance from the metal/oxide interface e.g. [Motta et al, 2005].

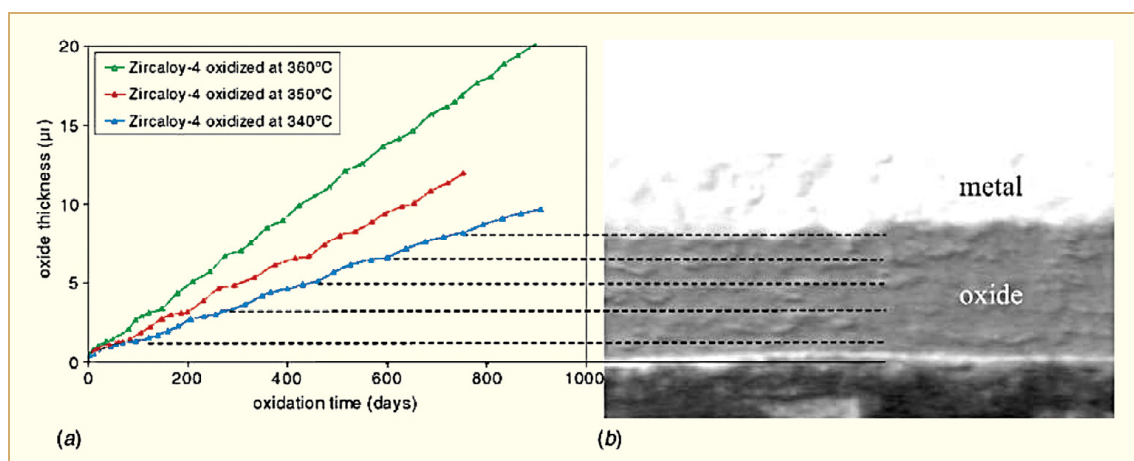


Figure 6-2: Corrosion of Zry-4 in autoclave at 340-360°C [Bonieau et al, 2007].

The post-transition oxidation rate is not always constant. [Hillner et al, 2000] found that the tested alpha annealed (RX) Zry-2 and Zry-4 exhibited first a lower linear post transition corrosion rate (stage 1) that increased at rather long exposure times, at a certain oxide layer thickness (10-40 µm), by a factor of 1.4-2.2 (stage 2). [Garzarolli et al, 1989a] have reported that such a late acceleration of the post transition corrosion rate occurs only for Zry-type alloys with a rather small SPP size. However, most Zr alloy cladding materials do not show such late corrosion acceleration.

The detailed corrosion behaviour depends on material and corrosion environment condition:

- In pure zirconium a corrosion breakaway occurs resulting in an unstable oxide growth at some point - green dashed curve in Figure 6-3.
- In corrosion-resistant zirconium alloys a rate transition occurs at a thickness of 2 to 5 μm , depending on material- red dashed curve in Figure 6-3.
- In pressurized water and high-pressure steam, repeated cycles with corrosion rate transitions can be seen for highly corrosion-resistant alloys, e.g. with $>0.3\%$ Fe continuing to the maximum times tested- black curve in Figure 6-3.
- However, in low-pressure steam the corrosion rate remains constant after the transition and is, on average, similar to that in high-pressure steam at the same temperature. In alloys with very fine SPP or with a high-Cr alloy content the corrosion rate accelerates after a certain oxide thickness: at least if tested in hydrogenated environments at high pressures - blue dashed curve in Figure 6-3.

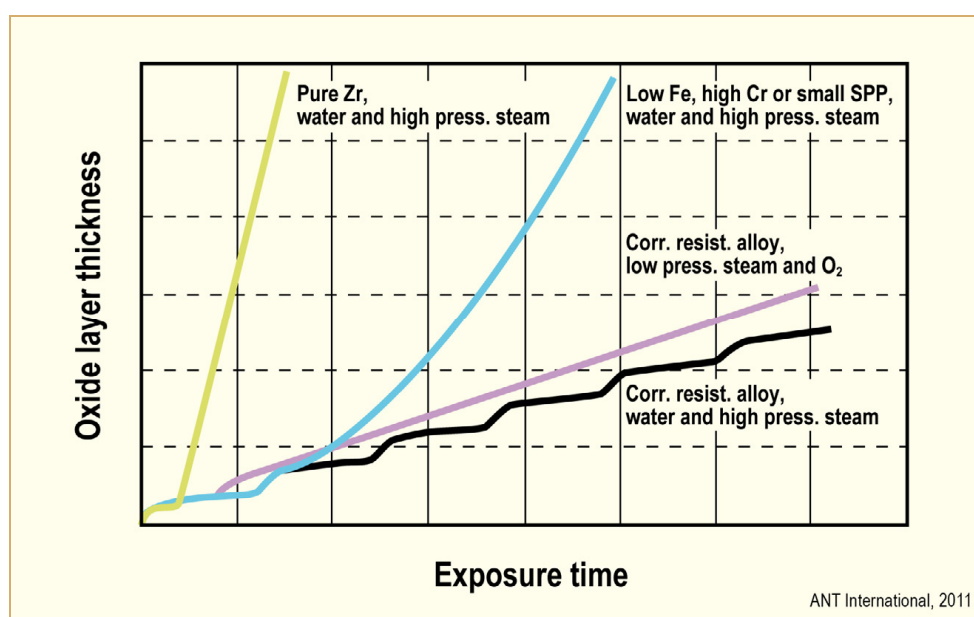


Figure 6-3: Principle corrosion behaviour of different materials in different environments [Adamson et al, 2007/2008].

Oxygen in the corrosion environment has not much effect on out reactor corrosion [Garzarolli et al, 1989a] but increases corrosion of ZrNb alloys significantly (see lower and upper black dashed curves in Figure 6-4). In high pressure (>70 bar) steam at $420-550^{\circ}\text{C}$ a localized corrosion, the so called nodular corrosion may appear in sensitive Zry-2/4 lots.

Irradiation increases corrosion in oxygenated coolant (BWR) especially at the early beginning (Figure 6-4). Furthermore, nodular corrosion may start in reactor after 10 to 100 days and shadow corrosion after a few days if a SS or Inconel component is close or in contact. At HBs, when the SPP are mostly dissolved by irradiation, uniform corrosion may accelerate (see red data points in Figure 6-4).

7 Primary failures and secondary degradation (Peter Rudling)

This section is focused on giving a comprehensive review of debris fretting mechanisms and remedies.

7.1 Debris fretting

7.1.1 Introduction

Debris fretting is still today one of the major, recurring causes of fuel failures in BWRs, PWRs, VVERs and CANDUs. Figure 7-1, Figure 7-2 shows the failure causes in PWR and BWR fuel worldwide from 1994 to 2006 done by International Atomic Energy Agency (IAEA) [IAEA, 2010a].

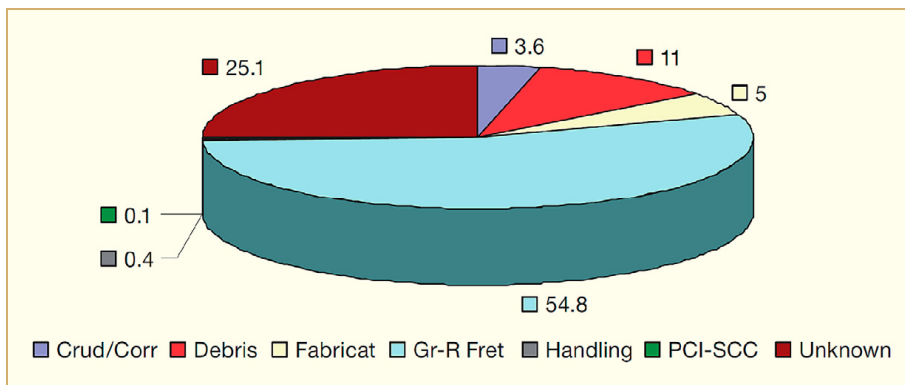


Figure 7-1: PWR fuel failure causes worldwide in 1994–2006 [IAEA, 2010a].

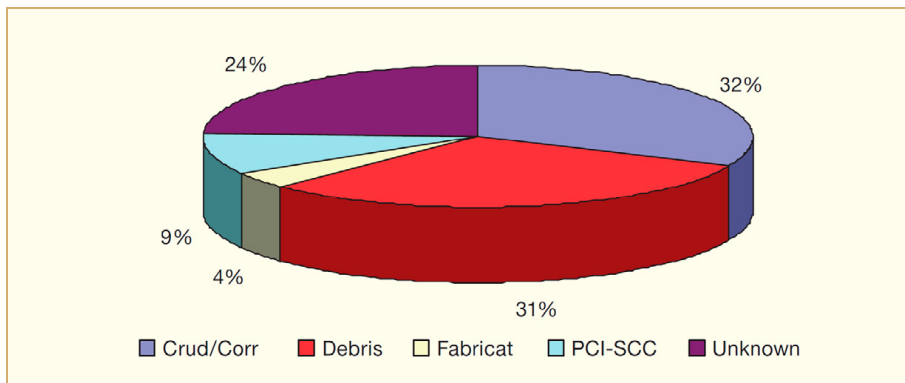


Figure 7-2: BWR fuel failure causes world distribution [IAEA, 2010a].

Table 7-1 and Table 7-2 shows more recent data.

Table 7-1: PWR failure rates (% of assemblies) [Adamson et al, 2010].

Failure cause	US (FRED) (2000-2009)	US (FRED) (2008-2010)	World wide (IAEA) (2003-2006)	EdF (1997-2008)	W
					(% plants with W fuel experiencing this failure type) (2008)
GTRF	77	77.1	52.1	42.8	9
Debris	5	5.6	9.3	5.9	7
Manufacturing	3	2.2	4.8	16.4	4
CRUD/Corrosion	2	1.8	0.0		
PCI	2	2.2	0.6		
Handling			0.0		
Unknown or not inspected	11	7.5	33.2	35.6	1

ANT International, 2011

Table 7-2: BWR failure rates (% of assemblies) [Adamson et al, 2010].

Failure cause	US (FRED) (2000-2009)	US (FRED) (2008-2010)	World wide (IAEA) (2003-2006)	GNF		W (2010)
				(2008 - mid 2010) US	Non-US	
Debris	39	20	27.8	100.0	67	89
PCI or duty	25		12.3		22	
CRUD/Corrosion	13		45.7			
Manufacturing	2		0.6			
Unknown or not inspected	21	80	13.6		11	11

ANT International, 2011

Debris fretting occurs when there is a mechanical interaction between debris and the cladding, which leads to a combination of corrosion and erosion that causes the impinging debris to wear through the cladding wall (Figure 7-3). Loose metallic debris can circulate in the reactor system and become trapped in the FA. The debris causing the fretting could either be already present in the assembly (from manufacturing) or be transported to the assembly by the coolant from other sources.

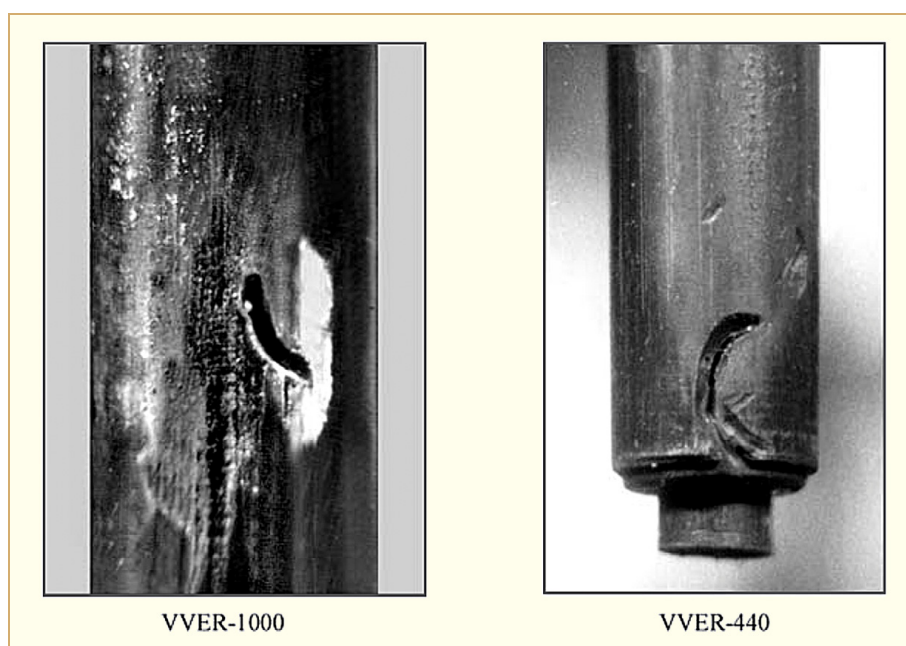


Figure 7-3: FRs failed due to debris fretting [Smirnov et al, 2005].

Typically, debris is trapped in a FA between FRs and spacers. In PWRs and VVERs, debris usually lodges in the bottom spacer and is exposed to the largest turbulence at this elevation due to the impact of the bottom nozzle to the coolant inlet flow. The debris particle will vibrate under the influence of the coolant flow and cause fretting holes within a few months in some cases. Debris failures have also been observed just above the Lower Tie Plate (LTP) in BWR FAs, but are not as common as in PWR/VVERs assembly bottom spacers.

The actual fretting debris is generally not found in, or adjacent to, the fretting hole produced. The whole shape is normally instead used to deduce the debris fretting as the primary failure cause. There should, nevertheless, always be a debris-fretting hole found to deduce debris fretting as a primary failure cause by definition. This is because the fretting hole should have an equally large, but generally larger, aspect at the cladding outer wall in relation to the penetration at the inner wall. There are other primary failure mechanisms that may produce small primary failures (mainly because they grow from the inside), sometimes impossible to find by visual inspection of the cladding surface. If the CRUD layer is thick, or the cladding oxide layer thick and spalling, debris-fretting holes can be hard to detect. The assessment if a fuel failure is due to debris fretting or other causes during operation and post-irradiation examinations are treated in Fuel Material Technology Report (FMTR) Vol. IV.

The observed debris typically includes turnings and shavings such as those from metal working operations performed during primary system maintenance or modifications, e.g. [Leroux, 2010]. In a few isolated cases, large objects such as tools, screws, bolts, nuts, metal clips, electrical connectors, pieces of lock wire and other wires, shavings from defective pumps or valves, parts of gaskets and saw blades have been found in damaged FAs. Small wires, turnings and chips appear to be the dominant source of debris fretting, however. A tendency for failures from debris fretting to occur early in life appears to exist, but needs to be evaluated based on the actual timing of a large number of such failures, see for example [Ryttersson et al, 2007].

8 Cladding performance under accident conditions LOCA and RIA

A limited amount of information was published on this topic during the last 18 months. Cladding performance under accident conditions LOCA and RIA will be covered in ZIRAT17/IZNA12 (next year).

9 Fuel performance during dry storage (Charles Patterson)

9.1 Introduction

Managed, recoverable storage of irradiated fuel continues to be an essential aspect of water-reactor fuel cycles throughout the nuclear community. As of the latest comprehensive survey (mid-2010), about 225 000 tons of used or (SNF)⁴¹ is being stored around world [Sokolov, 2010]. The inventory of SNF is increasing by about 6 800 tons per year. This fuel is being stored in pools located in reactor buildings or located away from reactors and in dry containers at reactor sites or at interim storage facilities. In general, wet and dry storage is occurring without major incidents. The exception is the apparent damage to fuel in reactor storage pools at the Fukushima Daiichi site following the Great Tohoku Earthquake and Tsunami in March 2011. This issue is mentioned here because of the potential for increased reliance on dry storage as proposed by the Transportation and Storage Subcommittee of the BRC on America's Nuclear Future [BRC, 2011d]. Managed storage is, however, only a temporary step in the overall fuel cycle; the fundamental issue post-storage processing and disposition of SNF and High-Level Waste (HLW) is being addressed differently among nuclear countries and remains unresolved other than agreement that geologic disposal is ultimately needed.

Approaches to the fuel cycle vary among countries with nuclear power programs [Kakodkar, 2010]. Many countries have explicitly or implicitly (by indecision) adopted an open fuel cycle, shown schematically in Figure 9-1, in which SNF will be disposed of in a permanent repository without recycling. Other countries have implemented or are developing recycling programs which are shown schematically in Figure 9-2 and Figure 9-3; e.g., Belgium, China, France, India, Japan, Russia and the United Kingdom. In all cases, capabilities for the final disposal of SNF and the related HLW are needed.

Currently, large scale, commercial repositories for SNF and HLW are unavailable. Most countries that generate nuclear power are in the process of developing criteria, designs and sites for the permanent disposal of SNF. As indicated in Table 9-1, however, operating repositories have yet to become licensed realities. Meanwhile the pools at the nuclear plant sites are filling with spent fuel and the utilities are transferring the spent fuel from the pools to dry cask storage sites that are located, mostly, at the plant sites but also at remote storage facilities. Exceptions to this practice are the central, large intermediate pool facilities that serve all the plants in Sweden (CLAB facility), all the plants in Finland (KPA-STORE), the fuel waiting reprocessing at La Hague, France and fuel from RBMK and VVER reactors in Russia. The lack of a licensed permanent fuel repository in any country has placed total reliance on intermediate storage. As a result dry storage has become a major activity and business component of current fuel strategies.

The importance of dry storage in back-end fuel strategies is due to a combination of factors. As noted above, the absence of permanent, geologic repositories combined with limited, in-pool storage capacity at reactor sites has forced the use of dry storage technology in countries that utilize a once-through, direct-disposal fuel cycle (Figure 9-1). Note that capabilities for interim storage will be needed even after permanent repositories become available because of storage limitations at existing reactor sites and likely constraints on decay heat in the repositories.

⁴¹ The term "Spent Nuclear Fuel" is used collectively in this report to refer to nuclear fuel that is described in literature and regulations as either "used" or "spent". In this case, SNF refers to irradiated fuel that will be stored in a recoverable manner prior to reprocessing or permanent disposal regardless of its initial, post-discharge disposition.

Table 9-1: Status of geologic repositories

Country	National decision	Status	Operational target date
Finland	Geological Repository	Site selected; licensing underway	2020
Sweden	Geological Repository	Site selected; licensing underway	2020
USA	Geological Repository	Waste Isolation Project operational ⁴² Yucca Mt. suspended in 2009 Policy and alternatives being discussed	Unknown
France	Geological Repository	Facility for HLW and transuranics under development	2025
Germany	Geological Repository		2030
Japan	Geological Repository		2030
Switzerland	Geological Repository		2040
UK	Geological Repository	Siting initiated Three communities interested	
Canada	Geological Repository	Siting initiated Eight communities possibly interested	≥2035
Belgium	No decision	R&D	R&D
Spain	No decision	R&D	R&D

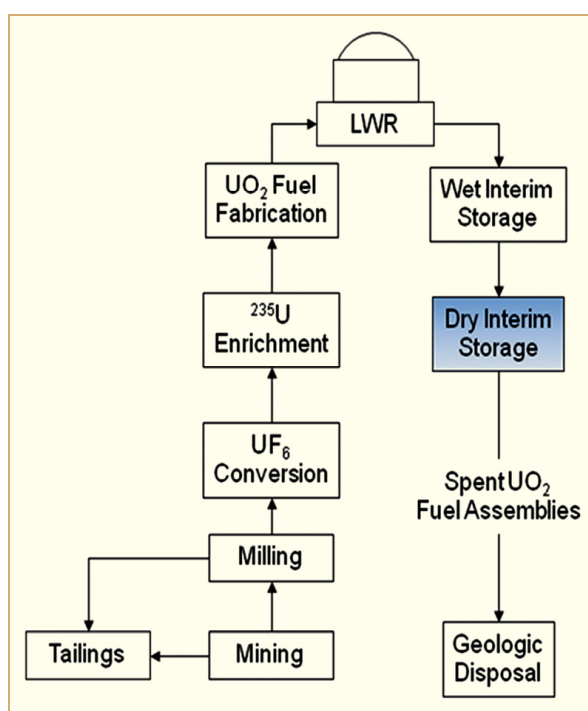


Figure 9-1: Schematic diagram of a once-through fuel cycle. LWR = Light water reactor, but also includes other thermal reactors.

⁴² The Waste Isolation Project in New Mexico, USA completed 12 year of successful operation in May, 2011. This facility is a geologic repository for transuranics and other HLW from military programs. It is not being used for commercial SNF.

Economic considerations and capacity imbalances also contribute to the storage of spent UO_2 fuel in countries that have commercial recycling capabilities. That is, dry storage offers a means of delaying reprocessing and recycling operations until the cost of fuel fabricated from virgin uranium or from highly-enriched, weapons-grade uranium justifies the recycling process. Dry storage also offers a means for balancing differences among the inventory of SNF, the capacity to reprocess irradiated fuel and the capacity to recycle the resulting plutonium as MOX fuel in the existing fleet of thermal-spectrum reactors.

It should be noted that, in the absence of permanent geologic repositories, dry storage is also an inherent element of a reprocessing fuel cycle. The build up of actinides such as neptunium, americium and curium typically limit recycling to a single pass through a light water reactor. As shown in Figure 9-2, this leads to the storage and disposal of spent, MOX assemblies in addition to the HLW that comes from the initial reprocessing operation. Recycled fuel generates more decay heat at a given discharge exposure than once-through fuel because of differences in the concentrations of radionuclides. Recycled fuel therefore requires longer decay time to reach the heat generation rates typically postulated for geologic storage. So, dry storage is common to both once-through and single-recycle fuel cycles.

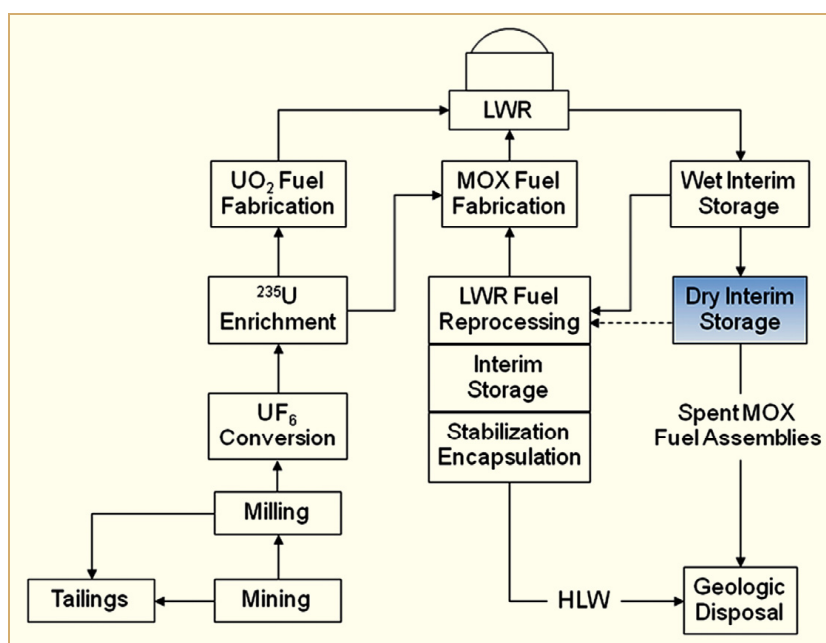


Figure 9-2: Schematic diagram of a once-through, reprocessing fuel cycle. HLW = Waste with high levels of radioactivity. MOX = Fuel consisting of mixed oxides of uranium and plutonium. LWR = Light water reactor, but also includes other thermal-spectrum reactors.

In principle, closed fuel cycles such as that shown in Figure 9-3 can eliminate the need for dry storage. But, the effects of reprocessing and recycling on storage and disposal depend strongly on the associated conditions or assumptions. As an example, reprocessing of spent fuel and the partitioning of transuranic nuclides (e.g., Pu, Np, Am, Cm), short half-life fission products (e.g., Cs, Sr) and long-lived fission products (e.g., Tc) have been predicted to reduce the volume of HLW by a factor of ten relative to the direct disposal of SNF [Pereira et al, 2006]. Alternately, the total volume of wastes after recycling was estimated in a recent study by the US Department of Energy (DOE) to be about the same as the corresponding, total volume of LWR fuel for an open fuel cycle [Carter et al, 2011]. Although this issue is the subject of ongoing investigations, the transmutation of transuranics and selected fission products from SNF by means of (fast) reactors with high-energy neutrons or accelerator-based devices is expected to convert these high activity products to stable or short-lived radionuclides. The overall effect of reducing the decay heat should allow for geologic disposal within a relatively short interval of time.

10 Trends and needs

Improved fuel reliability and operating economics are the driving forces for changing operating conditions, while at the same time maintaining acceptable margins to operating and regulatory safety limits. Table 10-1 gives the trends for BU achieved compared to regulatory limits in various countries. An approximate (“rule of thumb”) conversion of BU to fluence is 50 GWd/MT is equivalent to about 1×10^{22} n/cm², E>1MeV (or about 17 dpa), but this depends on many nuclear parameters such as enrichment, extent of moderation and neutron energy spectrum. In general PWRs operate to higher discharge BUs compared to BWR because of higher PWR power densities and neutron fluxes, but the differences are decreasing with time. There are some incentives to reach BUs of 60-70 GWd/MT batch average, but the economic values of doing so are decreasing. A majority of US plants and many in Europe have undergone power uprates, from a few percent to up to 20%. This increases the number of FAs in a core that operate at high power, thereby decreasing the margin to established limits. In cooperation with utilities, fuel suppliers have operated LTA or LUAs to very HB, in some cases approaching 100 GWd/MT peak rod exposure.

Table 10-1: Maximum BUs achieved vs. regulatory limits, (excludes LTAs).

Country	BU (GWD/MT)				Regulatory limit
	Batch	Assembly	Rod	Pellet	
USA	54	58	62	73	62.5 peak rod
Belgium		50-55			55 UO ₂ assy., 50 MOX assy.
Czech Republic	51	56	61		60 peak rod
Finland	45.6	46.5	53		45 assy
France	47	51 UO ₂ 42 MOX			52 assy
Germany	58	62	68		65 assy
Hungary		50	62		
Japan	50	55	62		55 UO ₂ assy., 45 MOX assy.
Korean Republic	46				60 rod
Netherlands	51.5	58	64.5		60 rod
Russia	60	65			
Spain	50.4	57.4	61.7	69	
Sweden	47	57.2	63.6		60 assy., 64 rod
Switzerland	58	60	65	71	80 pellet
Taiwan					60 rod (P), 54 assy. (B)
UK	44.3	46.5	50		55 pellet
Ukraine		50			

ANT International, 2011

As discussed in earlier sections as BU and fluence become higher, material properties and microstructure evolve. Examples include:

- In PWRs it is found the Zry-4 no longer meets corrosion and hydriding needs; therefore virtually all current PWR cladding use a zirconium alloy containing Nb.

- Although not a new phenomena, observed SPP dissolution and re-precipitation phenomena have required a new perspective on alloy development and HPU.
- BWR channel bow at HB has required a new understanding of the relationships between HPU, shadow corrosion and irradiation growth.

A broader listing of issues needing resolution include:

- Corrosion related to oxide thickness and H pickup:
 - BWRs and PWRs:
 - Mechanism of solid hydrides on corrosion mechanism.
 - Effect of Nb.
 - BWRs:
 - Shadow corrosion mechanisms and its relation to channel bow.
 - Late increased corrosion and HPU of Zry-2 at HBs.
 - CRUD-chemistry-corrosion interaction.
 - Effect of water chemistry impurities, as well as specific effects of NMCA, with or without Zn-injection.
 - PWRs:
 - Effects of surface contaminations and/or boiling on Zr-Nb alloys.
 - Welding of the new alloys may need improved processes (Zr-Nb alloys).
 - Effect of increased Li together with increased duty (subcooled boiling) with and without Zn-injection.
 - Effects of increased hydrogen coolant content (to mitigate Primary Water Stress Corrosion Cracking (PWSCC)).
 - Axial offset anomaly (AOA) mechanisms.
- Mechanical properties related to irradiation and H pickup:
 - Decreased ductility and fracture toughness as consequence of the increased HPU and formation of radial hydrides during any situation (e.g., RIA, PCMI, LOCA and post-LOCA events, seismic event, transport container drop-accident conditions).
 - Quantification of the effect of irradiation on solubility of hydrogen, and mechanism by which the phenomenon occurs.
 - Details of deformation mechanisms in zirconium alloys, including being able to predict the dislocation channelling system.
 - Development of micromechanical models applicable to deformation at appropriate component conditions.
 - DHC mechanism (degradation of failed fuel, outside-in cracking and dry storage).
 - Role and kinetics of Fe, Cr, Ni from dissolving SPPs in Zry and Zr-Nb alloys for corrosion, mechanical properties and dimensional stability.
- Dimensional stability:
 - Effect of hydrogen on irradiation growth mechanisms.
 - PWR FA bowing mechanism.
 - BWR fuel channel bowing mechanism and parameters affecting it such as: texture, residual stress, flux gradient, hydrogen gradient.

11 References

- Abolhassani S, Bart G. and Jakob A., *Examination of the chemical composition of irradiated zirconium based fuel claddings at the metal/oxide interface by TEM*, J. Nucl. Materials Vol. 399, pp. 1-12, 2010.
- Adamson R. B., *Cyclic Deformation of Neutron Irradiated Copper*, Phil. Mag. 17, pp. 681, 1968.
- Adamson R. B., *Effects of Neutron Irradiation on Microstructure and Properties of Zircaloy, Zirconium in the Nuclear Industry; Twelfth International Symposium, ASTM STP 1354*, pp. 15-31, West Conshohocken, PA, 2000.
- Adamson and Cox, *Impact of Irradiation on Material Performance*, ZIRAT10/IZNA5 Special Topics Report, ANT International, Mölnlycke, Sweden, 2005/2006.
- Adamson R., Cox B., Davies J., Garzarolli F., Rudling P. and Vaidyanathan S., *Pellet-Cladding Interaction (PCI and PCMI)*, ZIRAT11/IZNA6, Special Topics Report, ANT International, Mölnlycke, Sweden, 2006/2007.
- Adamson R., Garzarolli F., Cox B., Strasser A. and Rudling P., *Corrosion Mechanisms in Zirconium Alloys*, ZIRAT12/IZNA7 Special Topics Report, ANT International, Mölnlycke, Sweden, 2007/2008.
- Adamson R. B, Garzarolli F., Patterson C., Rudling P. and Strasser A., *ZIRAT14/IZNA9 Annual Report*, ANT International, Mölnlycke, Sweden, 2009.
- Adamson R. B, Garzarolli F., Patterson C., Rudling P. Strasser A. and Coleman K., *ZIRAT15/IZNA10 Annual Report*, ANT International, Mölnlycke, Sweden, 2010.
- Aitchison I. and Davies P. H., *Role of microsegregation in fracture of cold-worked Zr-2.5Nb pressure tubes*, J. Nucl. Mater., Vol. 203, pp. 206-220, 1993.
- Aksenov P. and Kolosovskiy V., *VVER Nuclear Fuel Fabrication Experience and Perspectives*, VVER Fuel Performance Conference, Helena Resort, Bulgaria, September, 2011.
- Alvarez R. et al., *Reducing the Hazards from Stored Spent Power Reactor Fuel in the United States*, Science and Global Security, 11, pp. 1-51, 2003.
- Alvarez-Armas I and Herenu S., *Influence of dynamic strain aging on the dislocation structure developed in Zircaloy-4 during low-cycle fatigue*, J. Nucl. Mater., Vol. 334, pp. 180-188, 2004.
- Amaev A. D., Anisomova J. A., Nikulina A. V., Saenko G. P., Sedova A. V and Fiveiskii M. B., *Corrosion of Zr alloys in boiling water under irradiation*, Proc. 4th U.N. Int. Conf. on Peaceful Uses of Atomic Energy, Geneva, CH, A/Conf.49/P/428, 1971.
- Ambartsumyan R. S., et al., *Mechanical properties and corrosion resistance of zirconium and its alloys in water, steam and gases at higher temperature*, Second International Conference on Peaceful Uses of Atomic Energy, Geneva, Paper N2049, 5:12-33, 1958.
- Amzallag C., *Environment Assisted Fatigue of Stainless Steels in PWR Environment*, ANTI LCC6 Seminar, 2011.
- Anada H. and Takeda K., *Microstructure of oxides on Zircaloy-4, 1.0Nb Zry-4, and Zircaloy-2 formed in 10.3-MPa steam at 673°C*, ASTM STP 1295, pp. 34-54, 1996.
- Aomi M. et al., *High Burnup Fuel Cladding Tube Property Testing for the Evaluation of Spent Fuel Integrity during Interim Dry Storage*, In Proceedings of an International Conference on Management of Spent Fuel from Nuclear Power Reactors, Vienna 19-22 June 2006, STI/PUB/1295, IAEA, pp. 409-423, Vienna, Austria, 2007.

- Aomi M. et al., *Evaluation of Hydride Reorientation Behavior and Mechanical Properties for High-Burnup Fuel-Cladding Tubes in Interim Dry Storage*, Journal of ASTM International, Vol. 5, Issue 9, Paper ID JAI101262, 2009.
- Arashi H. and Ishigame J. M., *Raman spectroscopy studies of the polymorphism in ZrO₂ at high stresses*, Phys. Stat. Sol. 71, 313, pp. 313-321, 1982.
- Armas A. F. and Alvarez-Armas I., *Cyclic Behavior of Zircaloy-4 at Elevated Temperatures*, Zirconium in the Nuclear Industry: Seventh Int'l Symposium, ASTM STP 939, R. B. Adamson and L. F. P. Van Swam, Eds., Am. Soc. for Testing and Materials, Philadelphia, 617-630, 1987.
- Armas A. F., Herenu S., Bolmaro R., and Alvarez-Armas, I., *Cyclic softening mechanisms of Zircaloy-4*, J. Nucl. Mater., Vol. 326, pp. 195-200, 2004.
- Asatiani I., Balabanov S. and Kuznetsov A., *Operational Results of WWER Fuel Fabricated by MSZ, (Elektrostal, Russia)*, VVER Fuel Performance Conference, Helena Resort, Bulgaria, September, 2011.
- ASM International, *Material Characterization*, ASM International, 1992.
- ASTM, *Standard Specification for Zirconium and Zirconium Alloy Ingots for Nuclear Application*, B 350/B 359M-11, 2011.
- Auger P., Pareige P., Akamatsu M. and Blavette D., *APFIM investigation of clustering in neutron-irradiated Fe-Cu alloys and pressure vessel steels*, J. Nucl. Mater. 225, pp. 225-230., 1995.
- Austin J. H. et al, J. Nucl. Mat. Vol. 51, p. 321, 1974.
- Avril J., *Encyclopédie Vishay d'analyse des contraintes*, Malakoff, Paris, France, 1974.
- Bahurmuz A. A., Muir I. J. and Urbanic V. F., *Predicting oxidation and deuterium ingress for Zr-2.5Nb CANDU pressure tubes*, ASTM STP 1467, pp. 547-562, (2005). Or J. ASTL international, Vol. 2, n°5, JAI 12342, May 2005.
- Barbérís P., Corolleur-Thomas G., Guinebretière R., Merle-Mejean T., Mirgorodsky A. and Quintard P., *Raman spectra of tetragonal zirconia: powder to Zircaloy oxide frequency shift*, Journal of Nuclear Materials, 288, pp. 241-247, 2001.
- Baur K. et al, *Electrochemical examinations in 350°C water with respect to the mechanism of corrosion-hydrogen pickup*, ASTM STP 1354, pp. 836-852, 2000.
- Beie H. J. et al, *Examination of the corrosion mechanism of Zr alloys*, ASTM STP 1245, pp. 615-643, 1994.
- Benjamin A. S. et al., *Spent Fuel Heatup Following Loss of Water During Storage*, USNRC, Washington, DC, USA, 1979.
- Bergman T., *De Analysi Ferri*, Opuscula Physica et Chemica, Vol. 3, Chapter 26, pp. 1-108, 1783.
- Berry E. B. et al., *Hydrogen pickup during aqueous corrosion of Zr alloys*, Corrosion Vol. 17, pp. 109t-117t, 1961.
- Birkbeck college, 2006, <http://pd.chem.ucl.ac.uk/pdnn/pdindex.htm#inst3>.
- Blake M., *US Capacity Factors: Staying Around 90 Percent*, Nuclear News, May, 2011.
- Bolmaro R. E., Signorelli J. W., Brokmeir H-G., Armas A. F., Herenú S. and Alvarez-Armas I., *Cyclic Softening Mechanisms of Zry-4 at Room Temperature: The Unlikely Influence of Texture Variations*, Scripta Materialia 51, 617-621, 2004.

- Bonieu V. et al, *A New Model to predict the oxidation kinetics of Zr alloys in PWR*, 15th ASTM Internat. Symp. On Zr in the Nucl. Industry, Sunriver, Or. USA, 2007.
- Borland R., *Preventing Legacy Debris Fuel Defects at Perry*, Workshop on Fuel Cladding Integrity Challenges by Foreign Materials, Orlando, Florida, USA, September 30, 2010.
- Bossis P. Lelievre G., Barberis P., Iltis X. and LeFebvre F., *Multi-Scale Characterisation of the Metal-Oxide Interface of Zirconium Alloys*, Proc. 12th Int. Symp. on Zr in the Nucl. Ind., ASTM-STP-1354, pp. 918-940, 2000.
- Bossis P., Thomazet J. and Lefebvre F., *Study of the Mechanisms Controlling the Oxide Growth Under Irradiation: Characterization of Irradiated Zircaloy-4 and Zr-1Nb-O Oxide Scales*, Zirconium in the Nuclear Industry: Thirteenth International Symposium: ASTM STP 1423, G. D. Moan and P. Rudling, Eds., ASTM International, pp. 190-221, West Conshohocken, PA, 2002.
- Bossis P. et al, *Comparison of the high burnup corrosion of M5 and Low-Tin-Zry-4*, ASTM STP 1467, pp. 494-524, 2006.
- Bossis P., Verhaeghe B., Doriot S., Gilbon D., Chabretou V., Dalmais A., Mardon J. P., Blat M. and Miquet A., *In PWR Comprehensive Study of High Burn-up Corrosion and Growth Behavior of M5 and Recrystallized Low-Tin Zircaloy-4*, 15th ASTM International Symposium: Zirconium in the Nuclear Industry – Sunriver, OR, June 25-27, 2007.
- Bossis Ph. et al., *Corrosion of M5[®] in PWRs: Quantification of Li, B, H and Nb in the oxide layers formed under different conditions*, 16th ASTM Zr Symposium, Chengdu, China, May 9-13, 2010.
- Bouvier P, Godlewski J. and Lucazeau G., J. Nuclear Mat. Vol. 300, pp. 118-126, 2002.
- BRC, *Blue Ribbon Commission on America's Nuclear Future*, Draft Report to the Secretary of Energy, U.S. Department of Energy, Washington, D.C., USA, 2011a.
- BRC, *Disposal Subcommittee, Report to the Full Commission*, Blue Ribbon Commission on America's Nuclear Future (BRC), Washington, D.C., USA, 2011b.
- BRC, *Reactor and Fuel Cycle Technology Subcommittee Report to the Full Commission DRAFT*, Blue Ribbon Commission on America's Nuclear Future (BRC), 2011c.
- BRC, *Transportation and Storage Subcommittee Report to the Full Commission*, DRAFT, Blue Ribbon Commission on America's Nuclear Future (BRC), Washington, DC, USA, 2011d.
- Brillant G., Gupta F. and Pasturel A., *Fission Products Stability in Uranium Dioxide*, Journal of Nuclear Materials, Vo. 412, P. 170-176, 2011.
- Brown C. A., J. Nucl. Eng. Int., pp 28, Nov. 1991.
- Broy Y., Garzarolli F., Seibold A. and Van Swam L. F., *Influence of transition elements Fe, Cr, and V on long time corrosion in PWRs*, Zirconium in the Nuclear Industry: 12th Int'l Symposium, ASTM STP 1354, pp. 609-622, G. P. Sabol and G. D. Moan, Eds., West Conshohocken, PA, 2000.
- Brun G. et al, *Cumulative Fatigue and Creep-Fatigue Damage at 350°C on Recrystallised Zircaloy-4*, Zirconium in the Nuclear Industry: Seventh International Symposium. ASTM STP 939, pp 597-616, 1987.
- Bryner J. S., *The Cyclic Nature of Corrosion of Zircaloy-4 in 633 K Water*, Journal of Nuclear Materials, Vol. 82, pp. 84-101, 1979.